

X.L. LI[✉]
W.F. XIANG
H.Y. JING
H.B. LU
Z.H. MAI

Time evolution of the microstructures of LaAlO₃ thin films grown on Si substrates

Beijing National Laboratory for Condensed Matter Physics, Institute of Physics,
Chinese Academy of Sciences, Beijing 100080, P.R. China

Received: 3 April 2006/Accepted: 20 April 2006
Published online: 1 June 2006 • © Springer-Verlag 2006

ABSTRACT The structure and stability of amorphous LaAlO₃ thin films deposited on Si substrates were investigated by an X-ray reflectivity technique. The results show that the film/substrate interface contains a La_xAl_yO_zSi layer and a SiO_x layer. X-ray reflectivity profiles showed a continuous change after the films were exposed to ambient air for six months at room temperature. The X-ray reflectivity simulations suggest a diffusion of La and Al (mostly La) from the LaAlO₃ layer to the La_xAl_yO_zSi layer. This process stopped after about six months, and then the films reached a relative equilibrium state. Moreover, post-air-exposure annealing at 300 °C in air atmosphere could not change the final distributions of La and Al along the normal to the film's substrate. On the other hand, the leakage-current density slightly decreases after annealing at 300 °C, which might be caused by the decrease of oxygen vacancies in the films.

PACS 61.10.Kw; 77.55.+f; 68.60.Dv

1 Introduction

Recently, high- κ gate dielectric materials have attracted great interest for replacing SiO₂; in fabricating an advanced scaled complementary metal oxide semiconductor (CMOS) device [1], a suitable material needs a high dielectric constant, a high permittivity, a low leakage current, a large band gap, a large conduction-band offset to Si and thermodynamic stability in contact with silicon. Al₂O₃, La₂O₃, ZrO₂, HfO₂ and their pseudobinary oxides are considered as potential high- κ materials [2–5]. When these materials are deposited on silicon substrates, an interface layer such as SiO_x or metal silicates is commonly formed [6–10]. The stability of high- κ dielectric materials is an important issue for applications.

LaAlO₃ is now expected as a most promising candidate material, because it has a steady interface and a good dielectric property [11]. Many authors have investigated the interface structure and thermal stability of LaAlO₃ films on silicon [12–14]. In our previous work, we investigated the microstructures of amorphous LaAlO₃ thin films [15]. In this

article, we further report the stability of LaAlO₃ thin films at room temperature and during annealing at 300 °C by an X-ray reflectivity (XRR) technique. A continuous change of the microstructures of LaAlO₃ thin films was found with time at room temperature. This phenomenon takes place for six months. A suitable structure and explanation is discussed.

2 Experiments

The LaAlO₃ films were deposited on 2-in-diameter, *n*-type (100) Si substrates by the laser molecular beam epitaxy (L-MBE) technique. Prior to film deposition, Si wafers were cleaned with acetone, alcohol and dilute HF solution to remove any native oxide layer, producing a hydrogen-terminated surface. The depositions of the LaAlO₃ films were carried out at an oxygen pressure of 0.1 Pa and a substrate temperature of 700 °C. High-resolution X-ray diffraction (HRXRD) was performed to confirm that the LaAlO₃ films are amorphous.

The XRR and HRXRD measurements were performed on a Bruker D8 Advance diffractometer at room temperature with Cu-K α radiation. The incident beam was confined by a 0.1-mm slit 300 mm before the sample. XRR profiles were collected several times for more than one year. The samples were held in desiccators at room temperature after each measurement.

It is well known that XRR provides a powerful and non-destructive tool to investigate microstructures of thin films, which is sensitive to the electron density and the interfacial roughness of each layer in a multilayer structure. The information of the multilayer structure such as the thickness and the interface roughness can be obtained by fitting the experimental data using a certain structural refinement model [16, 17].

3 Results and discussion

Figure 1 shows the X-ray reflectivity profiles of the sample measured at different time. The curve a was measured as soon as the sample was taken out from the epitaxial chamber, and the curves b, c, d and e were taken after 1, 2, 4 and 6 months, respectively. From Fig. 1 one can see that there are several broad peaks in these reflectivity curves. With the lapse of time, the periods and amplitudes of the peaks change greatly. This indicates that the structure of a LaAlO₃ thin

✉ Fax: +39-39-6881175, E-mail: xiaolong.li@mdm.infm.it

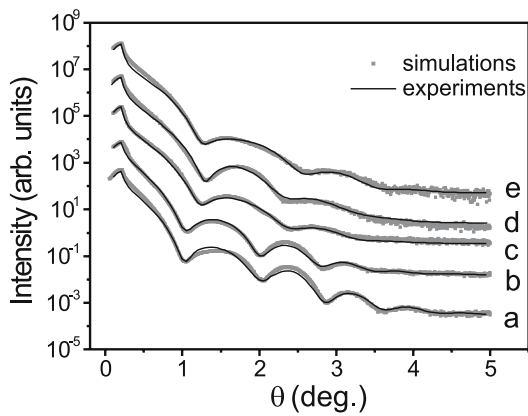


FIGURE 1 Time evolution of X-ray reflectivity profiles: the curve a is measured as soon as the sample was taken out from the epitaxial chamber; the curves b, c, d and e are measured after 1, 2, 4 and 6 months, respectively

film changes with time at room temperature. XRR simulations were performed to fit the experimental profiles based on the matrix method. The results of angle-resolved X-ray photoelectron spectroscopy show that the interface of LaAlO_3/Si is composed by a La-rich $\text{La}_x\text{Al}_y\text{O}_z\text{Si}$ diffusion layer and a SiO_x layer, which is reported elsewhere [17]. Based on these results, a three-layer model is constructed including a LaAlO_3 layer, a $\text{La}_x\text{Al}_y\text{O}_z\text{Si}$ diffusion layer and a SiO_x layer on top of the silicon substrate. During simulations, the $\text{La}_x\text{Al}_y\text{O}_z\text{Si}$ diffusion layer is indispensable, and a linear gradient of LaAlO_3 compound density is also considered. For a better fitting, the SiO_x layer is divided into two sub-layers with a low electron density layer and a high one. The low electron density layer corresponds to the amorphous SiO_2 and the high one is believed to correspond to quasiepitaxial growth of the SiO_2 near the substrate [18, 19], which is slightly denser than the Si substrate. The simulation parameters used are listed in Table 1.

From Table 1, one sees that the roughness of the $\text{La}_x\text{Al}_y\text{O}_z\text{Si}$ diffusion layer and the SiO_x layer is very large compared with the thickness of the two layers. It is well known that the roughness obtained from XRR fitting contains the physical roughness and the density variations. From the results of our former paper [15], the $\text{La}_x\text{Al}_y\text{O}_z\text{Si}$ diffusion layer is formed by the out diffusion of Si and the in diffusion of La and Al. It means that there would be a continuous change of the composition in the $\text{La}_x\text{Al}_y\text{O}_z\text{Si}$ diffusion layer. Hence, we conclude that the large roughness value is mainly caused by the density variations. It is obvious that the electron density of the LaAlO_3 layers varies greatly. For curve a, the electron density near the top surface of the LaAlO_3 layer is about $1.47 \text{ e}^-/\text{\AA}^3$, while it is about $0.82 \text{ e}^-/\text{\AA}^3$ in the vicinity of the substrate, indicating that the structure of the amorphous

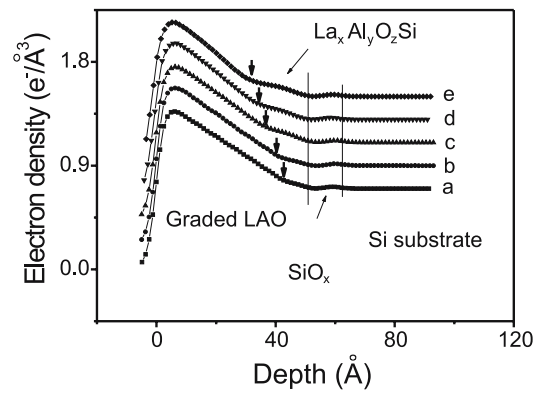


FIGURE 2 Comparison of electron density profiles (EDPs) with time. The arrows indicate the interface of the $\text{LaAlO}_3/\text{La}_x\text{Al}_y\text{O}_z\text{Si}$

ous LaAlO_3 film is highly inhomogeneous. It might be caused by the inhomogeneous depth distribution of La and Al in the LAO film; i.e. loosely packed in the vicinity of the substrate and relatively densely packed near the top surface. Since the electron density of LaAlO_3 bulk phase is about $1.69 \text{ e}^-/\text{\AA}^3$, there might be more defects near the bottom of the LaAlO_3 layer than near the top surface.

Comparing the five curves in Fig. 1 and the simulation parameters listed in Table 1, one sees that: (1) the thickness of the LaAlO_3 layer decreases from 47 \AA to 34 \AA after deposition for six months; (2) the thickness and the electron density of the $\text{La}_x\text{Al}_y\text{O}_z\text{Si}$ diffusion layer change from 3 \AA to 9 \AA and from $0.78 \text{ e}^-/\text{\AA}^3$ to $0.80 \text{ e}^-/\text{\AA}^3$, the root-mean-square roughness of the $\text{LaAlO}_3/\text{La}_x\text{Al}_y\text{O}_z\text{Si}$ interface changes from 3 \AA to 7 \AA ; (3) the thickness of the SiO_x layer and the roughness of the SiO_x/Si interface are almost unchanged. From the results mentioned above it is reasonable to assume that the La and Al species from the LaAlO_3 layer diffuse into the $\text{La}_x\text{Al}_y\text{O}_z\text{Si}$ layer to form a denser $\text{La}_x\text{Al}_y\text{O}_z\text{Si}$ layer and cause the increase of the $\text{LaAlO}_3/\text{La}_x\text{Al}_y\text{O}_z\text{Si}$ roughness, while almost no Si diffusion takes place in this process.

Figure 2 shows the electron density profiles (EDPs) of the sample with the passage of time obtained from the simulation data. The arrows indicate the interfaces of the $\text{LaAlO}_3/\text{La}_x\text{Al}_y\text{O}_z\text{Si}$, which are defined by the different density gradients of the two sides. One sees clearly that the arrows are moved toward the surface with time. It is the reason why La or Al species in the LaAlO_3 layer diffuse into the $\text{La}_x\text{Al}_y\text{O}_z\text{Si}$ layer as in the aforementioned discussion. Meanwhile, the results of angle-resolved X-ray photoelectron spectroscopy [15] show that the $\text{La}_x\text{Al}_y\text{O}_z\text{Si}$ layer is La-rich. Also, it is reported that La_2O_3 reacts more easily with Si than does Al_2O_3 [14]; therefore, the change of electron density with time is mainly contributed by the diffusion of La.

	LaAlO ₃	Interface layer ($\rho/d/\sigma$)			Si substrate
	$\rho_{\text{Top}} - \rho_{\text{Bottom}}/d/\sigma$	$\text{La}_x\text{Al}_y\text{O}_z\text{Si}$	SiO_x	Dense SiO_x	ρ/σ
Curve a	1.47 – 0.82/47/2.8	0.78/3/3	0.68/ 7/5	0.73/5/4	0.7/3
Curve b	1.47 – 0.82/44/2.8	0.78/4/4	0.68/ 8/5	0.73/5/4	0.7/3
Curve c	1.47 – 0.91/39/3.0	0.80/6/6	0.68/10/6	0.73/5/4	0.7/3
Curve d	1.47 – 0.91/36/3.2	0.80/8/6.8	0.68/10/6	0.73/5/4	0.7/3
Curve e	1.47 – 0.91/34/3.3	0.80/9/7	0.68/10/6	0.73/5/4	0.7/3

TABLE 1 Simulation data for fitting the small angle reflection curves: ρ is the electron density ($\text{e}^-/\text{\AA}^3$) ± 0.01 ; d is the layer thickness (\AA) ± 1 ; σ is the root-mean-square roughness of the interface (\AA) ± 0.5

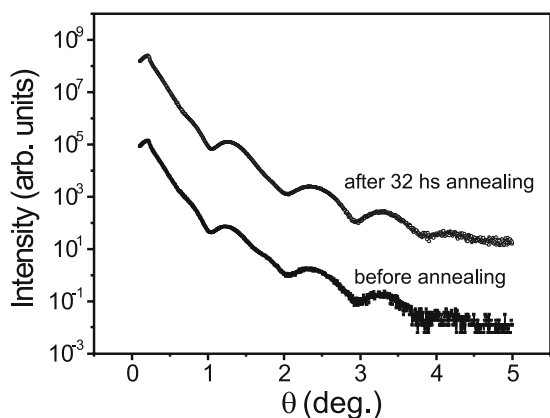


FIGURE 3 Comparison of the X-ray reflectivity profiles before and after 300 °C annealing

To affirm the time evolution of the microstructures, the XRR and HRXRD measurements were performed three times in another six months. To our surprise, the XRR curves did not show an obvious change with the curve e. Moreover, the LaAlO₃ film is still amorphous. The diffusion of La and Al from the LaAlO₃ layer to the La_xAl_yO_zSi layer stops after six months.

To further investigate the stability of the sample, annealing experiments were carried out in the atmosphere at 300 °C for 1 h, 8 h, 16 h and 32 h respectively for another sample deposited for one year. After annealing, the sample was subjected to XRR and current density–voltage (*I*–*V*) measurements. For the *I*–*V* measurement a Pt electrode was sputtered through a shadow mask with a diameter of about 1 mm to form a metal–insulator–semiconductor (Pt/LaAlO₃/Si) capacitor. Figure 3 shows the XRR profiles measured before and after 32-h annealing. One sees that the XRR profiles do not change significantly before and after annealing, indicating that the electron density of the film almost has not changed during annealing. Figure 4 shows the *I*–*V* characteristics of the film after different annealing times. Within the measurement errors, the leakage-current density slightly decreases after annealing. This might be due to the decrease of oxygen vacancies during annealing [11]. XRR is more sensitive to heavy rather than light elements. Therefore, the effects of the diffusion of light elements, like oxygen, on the total electron density cannot be detected with high efficiency. Since the XRR profiles exhibit almost no change after 300 °C annealing, we infer that there should be no diffusion of La or Al during the process.

Both La₂O₃ and Al₂O₃ have been reported to be thermodynamically stable in contact with silicon [20]. However, an interface sub-layer containing oxidized silicon is commonly observed. Mostly, the interface sub-layer formation occurs at the stage of film growth. LaAlO₃ films are reported to be stable after deposition, unless annealing at high temperature is applied [12]. However, our results suggest that La and Al (mostly La) diffuse from the LaAlO₃ layer to the La_xAl_yO_zSi layer already at room temperature. Film growth is therefore an inherently non-equilibrium process. Indeed, we showed that immediately after growth, the LaAlO₃ layer is highly inhomogeneous along the normal to the film's substrate, as far as the electron density is concerned. On the

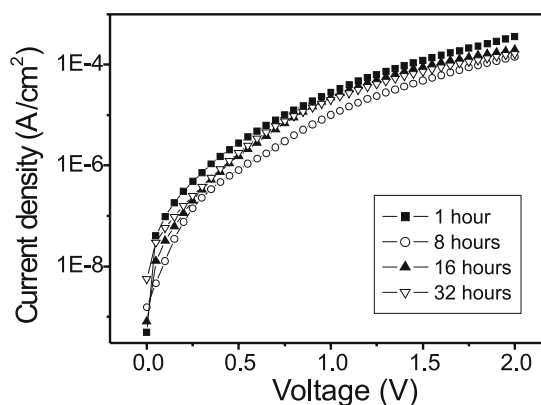


FIGURE 4 *J*–*V* curves of the sample with different annealing times at 300 °C

other hand, after about six months, the electron density inhomogeneity smooths out by adjusting the distribution of La and Al. Therefore, the films reach a relative equilibrium state.

4 Conclusions

In summary, an X-ray reflectivity technique was used to investigate the microstructures of amorphous LaAlO₃ films. Impressive results were found that with time evolution the thickness of the LaAlO₃ layer was thinned, while that of the La_xAl_yO_zSi layer was thickened at room temperature. We contributed this to the diffusion of La and Al (mostly La) from the LaAlO₃ layer to the La_xAl_yO_zSi layer. This process stopped after about six months, and then the films reached a relative equilibrium state. Moreover, post-air-exposure annealing at 300 °C in air atmosphere could not change the final distributions of La and Al along the normal to the film's substrate. On the other hand, the leakage-current density slightly decreases after annealing at 300 °C, which might be caused by the decrease of oxygen vacancies in the films.

ACKNOWLEDGEMENTS The work is supported by the National Natural Science Foundation of China (Grant Nos. 10274096 and 50072046). The authors wish to thank Dr. G. Scarel for helpful suggestions.

REFERENCES

- 1 G.D. Wilk, R.M. Wallace, J.M. Anthony, *J. Appl. Phys.* **89**, 5243 (2001)
- 2 E.P. Gusev, M. Copel, E. Cartier, I.J.R. Baumvol, C. Krug, M.A. Gribelyuk, *Appl. Phys. Lett.* **76**, 176 (2000)
- 3 K.J. Hubbard, D.G. Schlom, *J. Mater. Res.* **11**, 2757 (1996)
- 4 M. Copel, A. Gribelyuk, E. Gusev, *Appl. Phys. Lett.* **76**, 436 (2000)
- 5 H. Lee, L. Kang, R. Nieh, W.J. Qi, J.C. Lee, *Appl. Phys. Lett.* **76**, 1926 (2000)
- 6 S. Stemmer, J.P. Maria, A.L. Kingon, *Appl. Phys. Lett.* **79**, 102 (2001)
- 7 T. Gougousi, M.J. Kelly, D.B. Terry, G.N. Parsons, *J. Appl. Phys.* **93**, 1691 (2003)
- 8 M. Copel, E. Cartier, F.M. Ross, *Appl. Phys. Lett.* **78**, 1607 (2001)
- 9 M. Gurvitch, L. Manchanda, J.M. Gibson, *Appl. Phys. Lett.* **51**, 919 (1987)
- 10 M. Copel, *Appl. Phys. Lett.* **82**, 1580 (2003)
- 11 W.F. Xiang, H.B. Lu, L. Yan, H.Z. Guo, L.F. Liu, Y.L. Zhou, G.Z. Yang, *J. Appl. Phys.* **93**, 533 (2003)
- 12 B.E. Park, H. Ishiwara, *Appl. Phys. Lett.* **82**, 1197 (2003)
- 13 X.B. Lu, Z.G. Liu, Y.P. Wang, Y. Yang, X.P. Wang, H.W. Zhou, B.Y. Nguyen, *J. Appl. Phys.* **94**, 1229 (2003)

- 14 A.D. Li, Q.Y. Shao, H.Q. Ling, J.B. Cheng, W. Di, Z.G. Liu, N.B. Ming, C. Wang, H.W. Zhou, B.Y. Nguyen, *Appl. Phys. Lett.* **83**, 3540 (2003)
- 15 X.L. Li, W.F. Xiang, H.B. Lu, Z.H. Mai, *J. Appl. Phys.* **97**, 124104 (2005)
- 16 V. Nitz, M. Tolan, J.P. Schlomka, O.H. Seeck, J. Stettner, *W. Press, Phys. Rev. B* **54**, 5038 (1996)
- 17 M. Tolan, *X-Ray Scattering from Soft-Matter Thin Films* (Springer Tracts Mod. Phys.) (Springer, New York, 1999)
- 18 S.D. Kosowsky, P.S. Pershan, K.S. Krisch, J. Bevk, M.L. Green, D. Brasen, L.C. Feldman, P.K. Roy, *Appl. Phys. Lett.* **70**, 3119 (1997)
- 19 S. Banerjee, S. Chakraborty, P.T. Lai, *Appl. Phys. Lett.* **80**, 3075 (2002)
- 20 D.G. Schlom, J.H. Haeni, *MRS Bull.* **27**, 198 (2002)